Received: 7 November 2021 | Revised: 20 January 2022 | Accepted: 26 February 2022

DOI: 10.1002/bit.28075

ARTICLE

BIOTECHNOLOGY AND BIOENGINEERING WILEY

Bioprinting small-diameter vascular vessel with endothelium and smooth muscle by the approach of two-step crosslinking process

Qianheng Jin[1,2] | Guangzhe Jin[2] | Jihui Ju[2] | Lei Xu[1,2] | Linfeng Tang[2] | Yi Fu[3] | Ruixing Hou[2] | Anthony Atala[1] | Weixin Zhao[1]

[1]Wake Forest Institute for Regenerative Medicine, Wake Forest University School of Medicine, Winston-Salem, North Carolina, USA

[2]Department of Hand Surgery, Ruihua Affiliated Hospital of Soochow University, Suzhou, China

[3]Department of Human Anatomy, Histology and Embryology, School of Biology and Basic Medical Sciences, Soochow University, Suzhou, China

Correspondence

Ruixing Hou, Department of Hand Surgery, Ruihua Affiliated Hospital of Soochow University, 215104 Suzhou, China.
Email: hrx2020@suda.edu.cn

Anthony Atala and Weixin Zhao, Wake Forest Institute for Regenerative Medicine, Wake Forest University School of Medicine, Winston-Salem, NC 27157, USA.
Email: aatala@wakehealth.edu and wezhao@wakehealth.edu

Funding information

the National Natural Science Foundation of China, Grant/Award Number: 31900969; Suzhou Municipal Science and Technology Bureau, Grant/Award Number: SYS2020071; Suzhou Science and Education for Healthy, Grant/Award Number: KJXW2019073; the Gusu Health Talent Training Project of Suzhou, Grant/Award Number: GSWS2019088

Abstract

Three-dimensional bioprinting shows great potential for autologous vascular grafts due to its simplicity, accuracy, and flexibility. The 6-mm-diameter vascular grafts are used in clinic. However, producing small-diameter vascular grafts are still an enormous challenge. Normally, sacrificial hydrogels are used as temporary lumen support to mold tubular structure which will affect the stability of the fabricated structure. In this study, we have developed a new bioprinting approach to fabricating small-diameter vessel using two-step crosslinking process. The ¼ lumen wall of bioprinted gelatin mechacrylate (GelMA) flat structure was exposed to ultraviolet (UV) light briefly for gaining certain strength, while ¾ lumen wall showed as concave structure which remained uncrosslinked. Precrosslinked flat structure was merged towards the uncrosslinked concave structure. Two individual structures were combined tightly into an intact tubular structure after receiving more UV exposure time. Complicated tubular structures were constructed by these method. Notably, the GelMA-based bioink loaded with smooth muscle cells are bioprinted to form the outer layer of the tubular structure and human umbilical vein endothelial cells were seeded onto the inner surface of the tubular structure. A bionic vascular vessel with dual layers was fabricated successfully, and kept good viability and functionality. This study may provide a novel idea for fabricating biomimetic vascular network or other more complicated organs.

KEYWORDS

3D bioprinting, GelMA, small-diameter vascular vessel, tissue engineering, two-step crosslinking

Qianheng Jin and Guangzhe Jin contributed equally to this study.

1 | INTRODUCTION

Cardiovascular diseases (CVDs) are considered the major cause of death world widely (Zoghbi et al., 2014). The main treatment methods include medical therapy, endovascular intervention, and surgical transplantation (Buchanan et al., 2014). Autologous blood vascular transplantation remains to be the gold standard for surgical transplantation (Rodriguez et al., 2016). Although surgical technique continues to be improved, the success rate of autologous blood vascular transplantation is only around 50% (de Vries et al., 2016). The reason for failure is the embolization of vessels due to the difference of diameter and mechanical properties between grafts and cardiovascular (Y. Zhang et al., 2017). Tissue-engineered vascular grafts (TEVGs) have been explored as potential candidate for the treatment of CVDs. TEVGs, larger than 6 mm, have been widely used in cardiovascular surgery. However, due to the limitation of manufacturing technology, the construction of small-diameter blood vessels (SDBVs) grafts is still a challenge (Yamanaka et al., 2018).

Most of the vessels are composed of three concentric layers: intima, media, and adventitia (Elliott & Gerecht, 2016; Nemeno-Guanzon et al., 2012). Intima is the innermost layer of vessels, which is consisted of a monolayer of endothelial cells. It directly contacts the blood and is a barrier to prevent blood infiltration and thrombosis. The middle layer is composed of collagen I, collagen II, proteoglycan, elastin, and smooth muscle cells (SMCs). Smooth muscle and collagen are aligned in a spiral pattern which is conducive to maintaining the elasticity and structural support. The adventitia is composed of fibroblasts and a loose collagen structure, which can keep the vascular structure intact and prevent tearing (Lesman et al., 2016; Tomasina et al., 2019). There are many methods for making TEVGs, including electrospinning, phase separation, dissolution casting, and so on (Jing et al., 2015; Miller et al., 2012; Pattanaik et al., 2019; Wang et al., 2018). Those processes simulate blood vessels mostly in mechanical properties, which are still insufficient in biological properties.

Three-dimensional (3D) bioprinting, a newly developed technology that integrates digital modeling, electromechanical control, information control, biomaterials, and chemistry, can accurately locate the cells and biomaterials into the complex multiscale structure and simulate the complex tissue (Kolesky et al., 2016; Murphy & Atala, 2014). In the past decade, 3D bioprinting has been widely used in the field of vascular regenerative medicine (Hong et al., 2020; Kolesky et al., 2014). Rotary bioprinting is a convenient method. Fibrin-based vascular structures are fabricated through a new self-designed rotary 3D bioprinter. During 2 months of the cultures, mechanical strength and collagen deposition are observed and the burst pressure of the structure reaches 52% of human saphenous vein (Freeman et al., 2019). Yet, the structure constructed in this way is relatively immature, which cannot meet the complexity of natural vessels. A heterogeneous bilayer bionic blood vessels with 2 cm length and 4 mm lumen diameter are bioprinted by vertical stacking method in one step. The dense inner layer containing human umbilical vein endothelial cells (HUVECs) and the loose outer layer containing SMCs are formed by using the two separate concentrations of gelatin methacrylate (GelMA) in different layers (Xu et al., 2020). The above research provides a theoretical possibility for us to create small-diameter vessels. However, there is also an obvious deficiency in this study. The construct is easy to collapse during the printing process due to the gravity of hydrogels, thus the length and inner diameter of vessels are limited. Therefore, a new approach needs to be developed to overcome those shortcomings.

Sacrificial hydrogels, such as agarose, gelatin, and pluronic F127 are usually used to create complex tubular structure. Pluronic F127 containing HUVECs and Ca^{2+} is used as the coaxial inner layer, and catechol-functionalized, gelatin methacrylate (GelMA/C) containing SMCs is used as the coaxial outer layer. The GelMA/C undergoes rapid oxidative crosslinking in situ when touching the Ca^{2+} during the printing process and a vascular structure with high tissue affinity, perfusability, and permeability is formed (Cui et al., 2019). Agarose is applied as the temporary support of the scaffold and various vascular cell types are successfully self-assembled by a rapid prototyping bioprinting method to form a vessel construct with controllable diameter (Norotte et al., 2009). Although sacrificial hydrogels can be used as a support in the bioprinting process, each sacrifice hydrogel has its own disadvantages. Agarose has a melting point of 60–70°C which will lead the cell destruction in the process of removal (Miller et al., 2012). Gelatin has poor mechanical property and cannot fulfill the support of complex structure. Due to good quality in printing and wonderful support property, pluronic F127 is used commonly. However, the concentration of pluronic F127 used in the bioprinting needs to reach 30%–40% which will lead the water moving out of the low concentration bioink due to osmotic pressure. Thus, the accuracy of the structures and the cell viabilities will be affected (Wu et al., 2011).

We have developed a novel two-step crosslinking method for the fabrication of bilayer small-diameter vascular vessels, which could avoid the deficiency of sacrificial hydrogel and improve the accuracy of the printing process. To achieve this purpose, ¼ lumen wall of bioprinted GelMA-based flat structure was bioprinted and underwent a short-time UV light curing to obtain a certain strength. Then, the flat structure can be turned to cover the concave structure made by uncrosslinked GelMA to build a tubular structure. The tubular structure was treated with long-time UV curing to make sure that the two independent parts could be combined firmly in the format. First, we studied the properties of GelMA bioink with different crosslinking time, and then evaluated the connectivity of the two-step crosslinking structure. Furthermore, we fabricated complex small-diameter vascular vessels with HUVECs and SMCs by the two-step crosslinking method. To the best of our knowledge, this study represents a new methodology for constructing complicated bionic vascular vessel.

2 | MATERIALS AND METHODS

2.1 | Synthesis and identification of GelMA

The GelMA was synthesized by the following procedure (Xu et al., 2020). The 8 g gelatin (type A, 300 bloom from porcine skin;

Sigma-Aldrich) was dissolved in 50 ml 0.25 M carbonate-bicarbonate buffer with pH 9.2 for 1 h, and then 0.8 ml of methacrylic anhydride (MA) (Sigma-Aldrich) was slowly added into the gelatin solution. The mixture was allowed to react for 3 h under 700 rpm stirring at 55°C. The reaction was terminated by the addition of 80 ml Dulbecco's phosphate-buffered saline (DPBS), and the resulting solution was dialyzed in deionized (DI) water with 12–14 kDa cutoff dialysis tubes at 37°C for 7 days. The DI water was changed every 12 h. The solution was filtered and cooled at −20°C for 1 h, −80°C for 2 h, lyophilized for 5 days, and stored at −20°C freezer until use.

2.2 | ^{1}H-nuclear magnetic resonance analysis

GelMA was confirmed by ^{1}H-nuclear magnetic resonance (^{1}H-NMR). The 30 mg/ml GelMA was dissolved in deuterium oxide (D_2O) (Sigma-Aldrich) at 40°C. ^{1}H-NMR spectra were obtained by NMR spectroscopy with a single axis gradient at 400 MHz (^{1}H-NMR; Bruker). Gelatin was used as a control.

2.3 | Determination of 2,4,6-trinitrobenzenesulfonic acid

The methacrylation degree of GelMA was measured by 2,4,6-trinitrobenzenesulfonic acid (TNBS) (Sigma-Aldrich) assay. GelMA was dissolved in sodium bicarbonate solution (pH = 8.5, 0.1 M) to obtain a concentration of 200 µg/ml. The 250 µl of 0.01% (wt/vol) TNBS reaction solution was added to the sample solution and the reaction lasted for 2 h at 37°C. The reaction was terminated with 250 µl 10% sodium dodecyl sulfate and 125 µl 1 N hydrochloric acid (HCl). The 100 ml mixture was added into 96-well plate and optical density (OD) was obtained by microplate reader (SpectraMax M5; Molecular) at 335 mm. Gelatin was used as a control.

Degree of the methacrylation = (1−OD of GelMA/OD of Gelatin) × 100 (%).

2.4 | Fourier-transform infrared spectroscopy analysis

GelMA was dissolved in DPBS at a concentration of 50 mg/ml for 2 h at 37°C. After GelMA was completely dissolved, 1 m/v 2-hydroxy-4′-(2-hydroxyethoxy)−2-methylpropiophenone (irgacure 2959; Sigma-Aldrich) was added. The mixture was crosslinked for 5, 10, 20, 40, 60, 80, and 100 s with the wavelength of 365 mm and the intensity of 200 mV/cm^2 in the individual samples. The samples were lyophilized and analyzed by Fourier-transform infrared spectroscopy (FTIR)-attenuated total reflectance spectroscopy (Frontier; PerkinElmer). All samples were scanned five times at 400–4000 cm^{-1} with a resolution of 4 cm^{-1}. Gelatin was used as a control.

2.5 | Preparation sample of GelMA solutions

GelMA solutions consisted of 50 mg/ml GelMA, 30 mg/ml gelatin, 3.5 mg/ml sodium hyaluronate (hyaluronic acid [HA]), 10% vol/vol glycerol, and 1% m/v Irgacure 2959 in DPBS water. Gelatin and glycerol could increase the printability and HA could increase the biocompatibility of GelMA hydrogel (Xu et al., 2020). The 500 µl mixture was cast in a mold and crosslinked for 5, 10, 20, 40, 60, 80, and 100 s under the UV light with a wavelength of 365 nm and the intensity of 200 mV/cm^2 to make a sample with 1.8 cm in diameter and 2 mm in thickness in the individual samples.

2.6 | Rheological measurements

The mechanical properties of GelMA with different crosslinking times were analyzed by using a discovery hybrid thermometer dhr-2 (TA Instruments). Frequency scanning was performed from 1 to 100 Hz with 1% constant strain. Strain scanning was performed from 0.01% to 3% rad/s at an oscillation frequency of 1 Hz.

2.7 | Swelling ratio and residual mass test

GelMA samples with different crosslinking times were weighed as (Wo) and gently shaken in DPBS and DI water at 37°C for 2 days to remove the uncrosslinked GelMA. The swelling mass was recorded as (Ws) and the expanded samples were lyophilized to obtain the mass (Wr)

Swelling ratio = (Ws−Wr)/Wr × 100%,

Residual ratio = Wr/(500 × 5%) × 100%.

2.8 | Scanning electron microscopy

The samples were placed in DI water at 37°C for 2 days, cooled at −80°C for 2 h, and then lyophilized. The cross section of the structure was sputter coated with gold at 15 mA for 2 min (EM Ace600; Leica) and observed under a scanning electron microscope (SEM; Flex SEM1000; Hitachi) at 10 kV. The diameters of different samples were analyzed using Image J.

The 3D bionics vascular structure was fixed with 2.5% glutaraldehyde (Sigma-Aldrich) at 4°C for 4 h after 7 days of culture. The structure was dehydrated with 30%, 50%, 70%, 80%, 90%, 95%, and 100% ethanol for 20 min each. After replacing the ethanol with Co_2 by a critical point dryer (Leica; EM CPD 300) and coating with gold, the samples were observed by SEM.

2.9 | Combination of two step crosslinking

GelMA solution was added to one side of the mold (Figure 3a). After crosslinked for 10 s, the solution was added to the other side and

crosslinked for 100 s to form a two-step crosslinked sample. GelMA solution was added to both sides of the mold and directly crosslinked for 100 s was used as one-step crosslinked sample as a control.

Two-step crosslinked and one-step crosslinked samples were loaded in Instron mechanical tester (Model 5533; Instron Corporation), and tensile tests were conducted with a maximum value of 10 N load cell.

Two-step crosslinked samples were observed by SEM to analyze the pore size and the integrity of connections.

2.10 | Cell culture

HUVECs (Lonza) were cultured in endothelial cell growth medium 2 (EGM-2) (Lonza) and SMCs (Lonza) were cultured in SMC growth medium 2 (Promocell). Both media were added with 1% vol/vol penicillin and streptomycin and the cells were cultured at 37°C, 5% CO_2, and 95% relative humidity. The EGM-2 and SMC growth medium were mixed at 1:1 ratio for culturing the printed vascular structure, and the mixed medium was changed every 2 days. HUVECs and SMCs used in all experiments were in 4–8 generations.

2.11 | 3D bioprinting of vascular structure

3D bioprinting was conducted with a custom-made integrated tissue and organ printing. In brief, the printer had a *X*-, *Y*-, and *Z*-stage controllers, a distributing pneumatic pressure control system for accurately dispensing several materials within a single print. The bioprinter sat in a closed chamber under control temperature and humidity. It could deposit cell-laden hydrogels together with synthetic polymers and overcome the limitations on the size, shape, and structural integrity of single hydrogel prints and create customizable tissue.

For printing our constructs, we added 5% GelMA solution into the syringe with the nozzle of 300 μm (Izumi). The flat structure and the concave structure were printed with the pressure of 100 kPa and the feed rate of 60 mm/min. We crosslinked the flat structure under UV light for 10 s to increase mechanical strength, then placed it on top of concave structure, and this integrated structure was crosslinked for 100 s to make the two individual structures combined unitedly (Figure 3e).

The 10×10^6 SMCs were mixed into 5% GelMA solution, and then the cell-landen GelMA was bioprinted to fabricate the bionic vascular structure as described above. Before the seeding process, 50 μg/ml fibronectin (Invitrogen) solution was injected into the channel of the tubular construct to improve cell adhesion. The HUVECs suspension (30×10^6 cell/ml) was slowly injected into the lumen by 10 μl mircropipet to ensure that the cell suspension fills the entire space of the lumen. Then, the structures were incubated at 37°C for 2 h and were flipped every 30 min to permit cell attachment on all sides of the lumen. Nonadherent cells were gently removed out of the lumen and the structures were washed with DPBS for three times to maintain the patency of the lumen. A bionic small blood vessel with a monolayer of HUVECs and SMCs layer was completed after cultivation in the mixed medium for 7 days. (Freeman et al., 2019).

2.12 | Cell viability and proliferation

The cell viability was assessed using a LIVE/DEAD and Viability/cytotoxicity Kit (Invitrogen). Briefly, the vascular structure was washed three times with DPBS, and then incubated at 0.5 μl/ml Calcein AM and 2 μl/ml ethidium homodimer for 45 min. Laser confocal microscopy (LSI; Leica) was used to observe the living and dead cells in the structure. Six random views were selected to evaluate the cell viability using Image J.

Cell Counting Kit-8 (CCK-8; Sigma-Aldrich) was used to detect the cell proliferation in the vascular structure. These vascular structures were transferred into a 24-well plate. The 900 μl fresh medium and 100 μl CCK-8 solution were added. After incubated at 37°C for 3 h, 100 μl solution was transferred into 96-well plate and the ODs were read by spectramax M5 at 460 nm.

2.13 | Histological and immunofluorescence analysis

The vascular structures were fixed with 4% vol/vol paraformaldehyde after culture for 7 days and cut into 15 μm section with a cryostat (CM1950; Leica) at −20°C. Slices were stained with hematoxylin and eosin (H&E) and Masson's trichrome methods. Images were collected by light microscopy (DM4000b; Leica).

For immunofluorescence staining, HUVECs were labeled with mouse anti-human CD31 (1:50; Abcam) and SMCs were labeled with rabbit anti-human α-smooth muscle actin (α-SMA) (1:200; Abcam). Alexa Fluor 488 goat anti-mouse (1:500; Abcam) and Alexa Fluor 594 Donkey anti-rabbit (1:500; Abcam) were used as secondary antibodies. All the sections were counterstained with 4′,6-diamidino-2-phenylindole. Fluorescence images were obtained with a fluorescent microscope (Leica; DM8000). The sections without primary antibody staining were used as control.

2.14 | Statistical analysis

Data were processed by calculating means ± standard deviation. *T*-test was used to assess the differences between groups. $p < 0.05$ means significant difference ($^*p < 0.05$; $^{**}p < 0.01$; $^{***}p < 0.001$; NS, not significant)

3 | RESULTS

3.1 | Synthesis and identification of GelMA

The amino groups on gelatin were partly replaced by methacrylic acid to form GelMA with crosslinking ability (Bahcecioglu et al., 2019). The

synthetic GelMA was identified by ^{1}H-NMR (Figure S1). The characteristic resonance peak of the methacrylic acid group (5.5–6 ppm) appeared in GelMA, which is missing in the control. The substitution degree of GelMA was assessed to be 79.3% ± 2.7% by TNBS (Figure 1).

3.2 | The effect of crosslinking time on GelMA properties

The number of double bonds in GelMA increased with increasing crosslinking time (Chen et al., 2012) (Figure 2a). Treated with different crosslinking time, GelMA showed different physical states. While the GelMA with only 5 s crosslinking time was changed from liquid to preliminary solid, which cannot maintain its shape for a longer time. However, samples with 10, 20, and 40 s crosslinking time maintained good shape (Figure 2b) lasting for a longer time.

FTIR was used to identify the correlation peaks in GelMA with different crosslinking times. A peak at 1525 cm^{-1} corresponded to C–N stretching and N–H bending; 1640 cm^{-1} to O–H bonding; 2922 cm^{-1} to C–H stretching; and 3300 cm^{-1} to O–H stretching. GelMA with different crosslinking times showed different peaks at these positions (Dursun Usal et al., 2019). We evaluated the FTIR of gelatin, uncrosslinked GelMA, and GelMA with different crosslinking times. The peaks of the two amino groups at 1540 and 1640 cm^{-1} in uncrosslinked GelMA were significantly increased compare with gelatin, which indicated that the amino groups in gelatin were successfully replaced by methacrylic acid. After UV irradiation for different times, the two peaks gradually decreased. In addition, the –OH stretching vibrations at 3300 cm^{-1} also decreased, which was related to the decrease of total –OH caused by UV curing (Figure 2c).

GelMA with different crosslinking time was shaken in DI water at 37°C for 2 days. The uncrosslinked GelMA was removed, and the remaining GelMA in the structure expanded which led to the pore size increasing (Figure 2d). The average pore sizes were 292.2 ± 25.00 (5 s), 308.9 ± 23.53 (10 s), 175.8 ± 15.66 (20 s), 85.06 ± 8.977 (40 s), and 82.07 ± 9.089 (100 s) (Figure 2e). Gelatin, glycerin, and HA contained in crosslinked GelMA bioink will not affect the pore sizes of the constructs (Figure S2).

To characterize the physical properties of GelMA bioink with different crosslinking times, oscillatory rheological measurements were used. The storage modulus (G′) and viscosity coefficient of GelMA bioink increased with the crosslinking time, while it kept steady when the crosslinking time reached 40 s (Figure 2f,g). In a certain range, the storage modulus remained stable with changing of frequencies and strains, which indicated the structure of crosslinked GelMA was stable under the shear force (Figure 2h,i). In addition, the storage modulus of GelMA bioink at each crosslinking time was much greater than the loss modulus which indicated that crosslinked GelMA was in a solid state (Figure 2j).

GelMA bioink with different crosslinking times showed different swelling ratios in DPBS and DI water. GelMA's swelling ratio was 23 times in DPBS with 5 and 10 s crosslinking times. With increasing of crosslinking time, the swelling ratio decreased. The swelling ratio was 17.5 times with 20 s crosslinking time, and it was 15 times with 40 s at which point it stabilized (Figure 2k). The swelling ratio was more remarkable in DI water. The swelling ratio was 400 times in 5 and 10 s, 200 times with 20 s, and closed to 100 times with 40 s (Figure 2l). This trend indicated that an increased number of double bonds result in a more stable framework.

The residual mass indicated the amount of residual GelMA in structure. With the increased of crosslinking time, residual mass increased gradually. The average residual masses obtained were

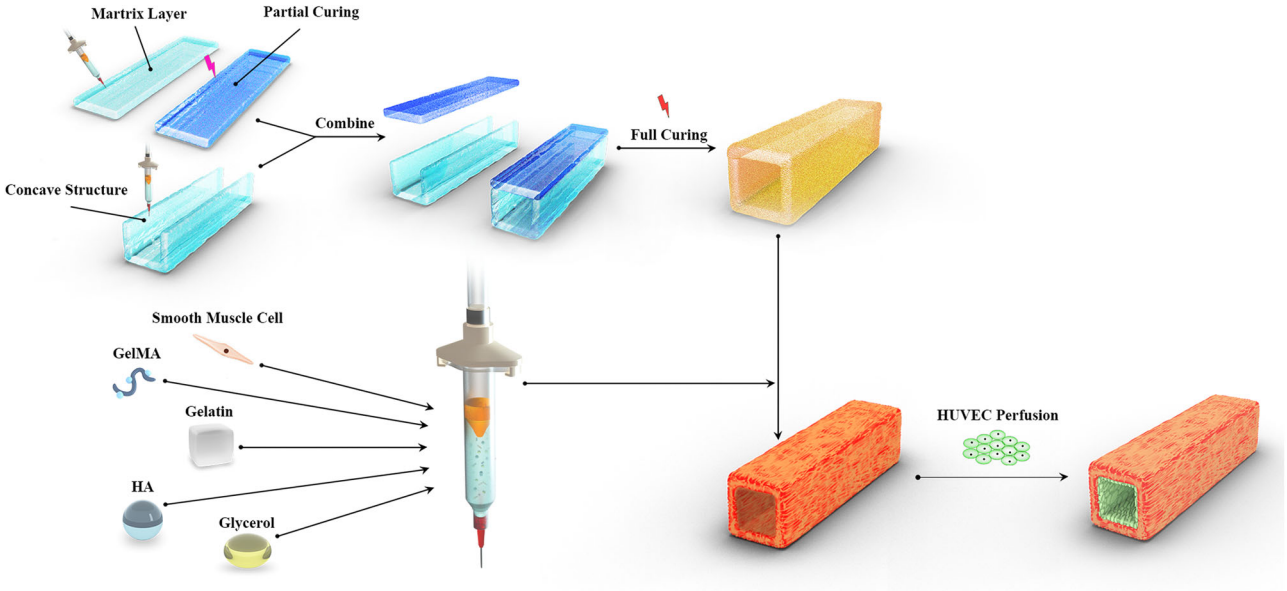

FIGURE 1 Schematic showing the novel printing method to create a small-diameter tubular construct and the process of bioprinting a bionic vascular. GelMA, gelatin mechacrylate; HA, hyaluronic acid; HUVEC, human umbilical vein endothelial cell

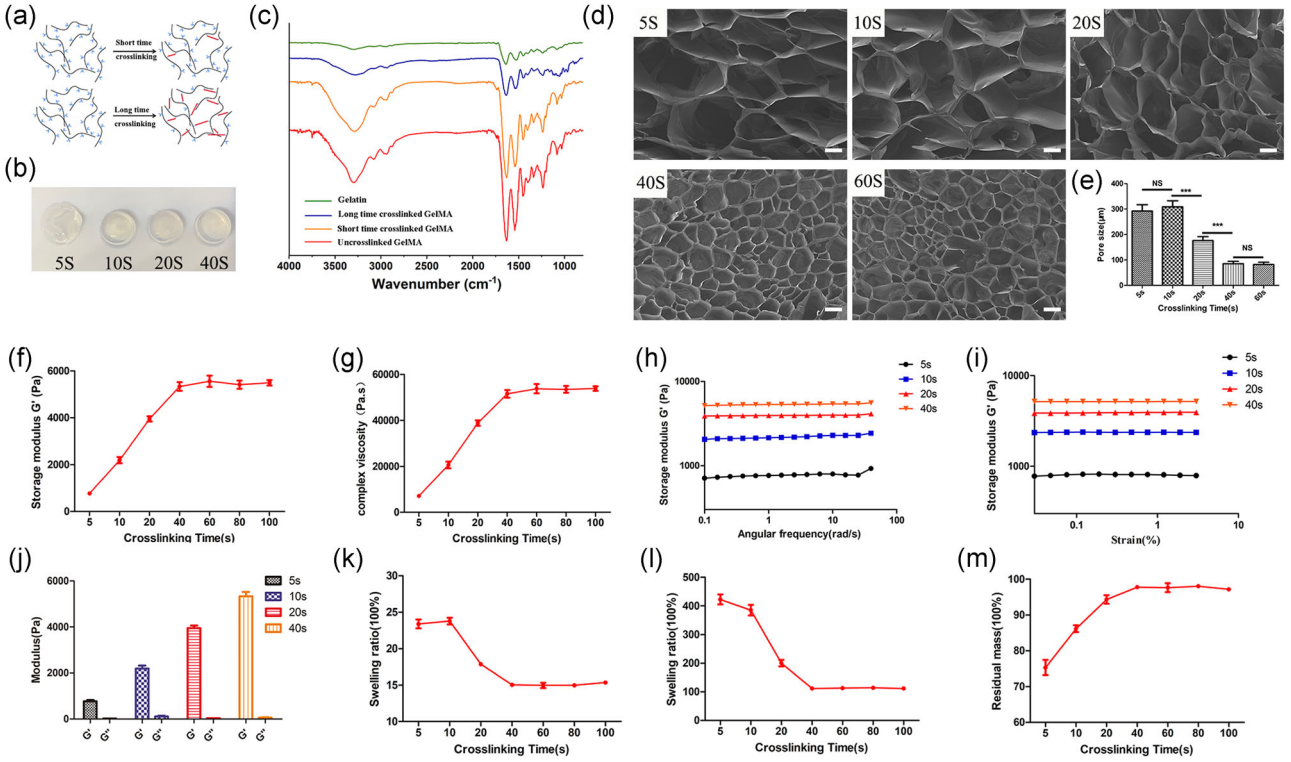

FIGURE 2 The analysis of GelMA hydrogel with different crosslinking times. (a) Schematics of GelMA polymer structure connections with different crosslinking times. (b) Gross images of GelMA with different crosslinking time. (c) FTIR of GelMA, long-time crosslinking GelMA, and short-time crosslinking GelMA. (d) The SEM of the GelMA samples at 5, 10, 20, 40, and 60 s crosslinking time. (e) Pore size assessment of the GelMA samples at 5, 10, 20, 40, and 60 s crosslinking time (***$p < 0.001$). Scale bar = 150 μm. (f, g) Storage modulus and complex viscosity of the GelMA samples at different crosslinking times. (h, i) The storage modulus of the GelMA samples at different crosslinking times varying with angular frequency and strain. (j) The comparison of storage modulus and loss modulus of the GelMA samples at 5, 10, 20, and 40 s crosslinking time. (k, l) The swelling ratio of the GelMA samples at different crosslinking times in DPBS and DI water. (m) The residual mass of the GelMA samples at different crosslinking times ($n = 6$). DI, deionized; DPBS, Dulbecco's phosphate-buffered saline; FTIR, Fourier-transform infrared spectroscopy; GelMA, gelatin mechacrylate; NS, not significant; SEM, scanning electron microscope

68.47% ± 3.85% (5 s), 78.32% ± 1.72% (10 s), 85.77% ± 2.11% (20 s), 88.90% ± 0.80% (40 s), 88.77% ± 2.22% (60 s), 80 s is 89.13% ± 0.09% (80 s), and 88.49% ± 1.58% (100 s) (Figure 2m).

3.3 | Combination of two-step crosslinking approach

Two-step crosslinking resulted in substantial cohesion. Figure 3a showed that 10 s precrosslinked GelMA can be recrosslinked with the uncrosslinked GelMA bioink and formed a united combination. There was no sign of splitting at the combining site under the SEM observation (Figure 3b). In tensile loading, there was no significant difference in Young's modulus and tensile strain between structures formed by one-step and two-step crosslinking methods ($p > 0.05$) (Figure 3c–e).

3.4 | Fabrication of complicated tubular structures

We used the two-step crosslinking approach to fabricating a tubular structure of GelMA. The method of two-step crosslinking to construct tubular structure was showed in Figure 3f. Figure 3g showed the tubular construct with different diameters (0.08–0.2 mm in lumen diameter and 0.6 mm in wall thickness). A 6 mm long tubular construct was showed in Figure 3h. SEM showed that the tubular structure has good bonding properties (Figure 3i).

Complicated designs demonstrated the advantages of two-step crosslinking method. We printed multiple curved tubular structure, branched tubular structure, circular tubular structure with single inlet/outlet, and several letters (Figure 4). Red inks were injected into these structures to show the connected channels within each structure and to demonstrate their integrity of fluid flow.

3.5 | Cellular vessel structures

The GelMA mixed with SMCs was used as the bioink for building vascular wall, while HUVECs were perfused into the inner vascular cavity to form a bionic barrier between the blood flow and vascular wall.

The viabilities of SMCs and HUVECs in the vascular structure were analyzed by live/dead staining. The fluorescence images of 1, 4,

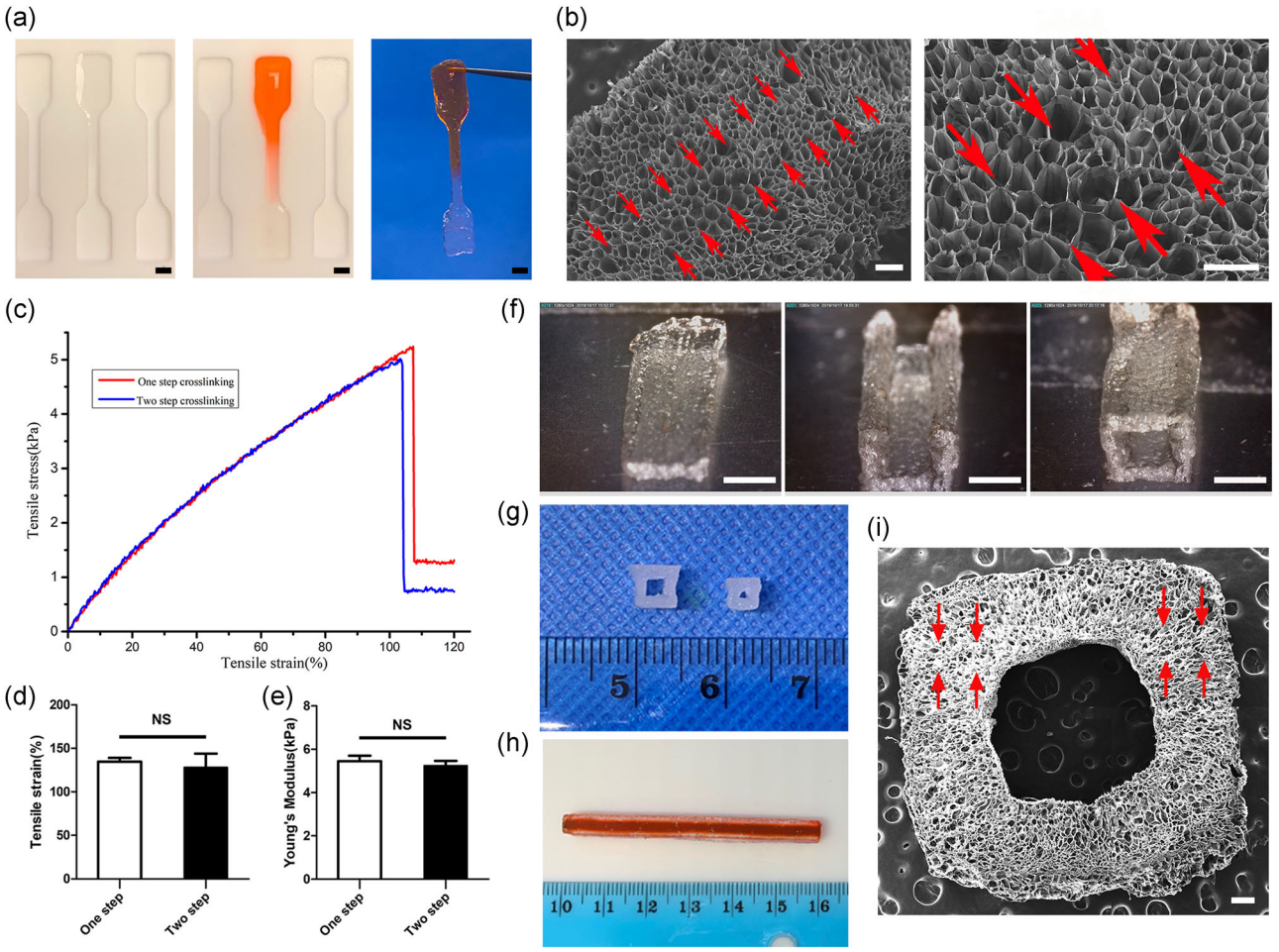

FIGURE 3 The combining site of the samples with two-step crosslinking method and the appearance of tubular structure. (a) Gross image of the construct made by two-step crosslinking. Scale bar = 2 mm. (b) The SEM of the construct made by two-step crosslinking (the red arrow refers to the combining site). Scale bar = 200 μm. (c) The stress–strain curves of one-step crosslinking structure and two-step crosslinking structure. (n = 6). (d, e) The tensile strain and Young's modulus of one-step crosslinking structure and two-step crosslinking structure. (n = 6). (f) The process of constructing a tubular structure. Scale bar = 2 mm. (g) The tubular structures with different diameter. (h) 6 cm length tubular structure. (i) SEM of tubular structure (the red arrow refers to the combining site). Scale bar = 200 μm. NS, not significant; SEM, scanning electron microscope

and 7 days were obtained by confocal microscope. The cells were in granular state at the first day after printing. On the fourth day, the number of cells began to increase, and some cells began to expand in their shape. Most cells expanded and SMCs showed the long spindle shape in 7 days (Figure 5a). The cell survival rates were 93.64 ± 1.455 (Day 1), 91.62 ± 2.070 (Day 4), and 95.62 ± 1.312 (Day 7). All the survival rates in the structures were more than 90% (Figure 5b). CCK-8 was used to analyze cell proliferation. The CCK-8 absorption values of HUVECs and SMCs on Days 0, 1, 4, and 7 were 0.110 ± 0.0138, 0.110 ± 0.0068, 0.209 ± 0.0121, and 0.315 ± 0.0179, respectively (Figure 5c). Cells significantly proliferated in the vascular structures.

H&E and Masson's trichrome staining were used for morphological detection, and immunofluorescence was used for functional assessment. After 1 week of culture, spreading out SMCs were well distributed in the outer layer. HUVECs formed a monolayer cell coverage on the inner lumen surface (Figure 5d,e). CD31 and α-SMA immunofluorescence confirmed an inner endothelial layer and the outer smooth muscle layer from the vascular structure (Figure 6a).

The morphology of the outer, middle, and inner layers of GelMA vascular construct were further observed by SEM. Interestingly, the SMCs in the outer layer and middle layer were spreading out and arranged linearly along the vertical direction of printing. The HUVECs in the inner layers attached tightly to the GelMA lumen surface and expanded to form a tight barrier evenly (Figure 6b).

4 | DISCUSSION

Scientists have been rapidly developing tissue-engineered artificial blood vessels in the past decade, and used multiple ways to construct them (Morin et al., 2013). 3D bioprinting has become a research hotspot because of precision spatial control and uniform cell distribution (Hong et al., 2020). 3D bioprinting is a rapid prototyping

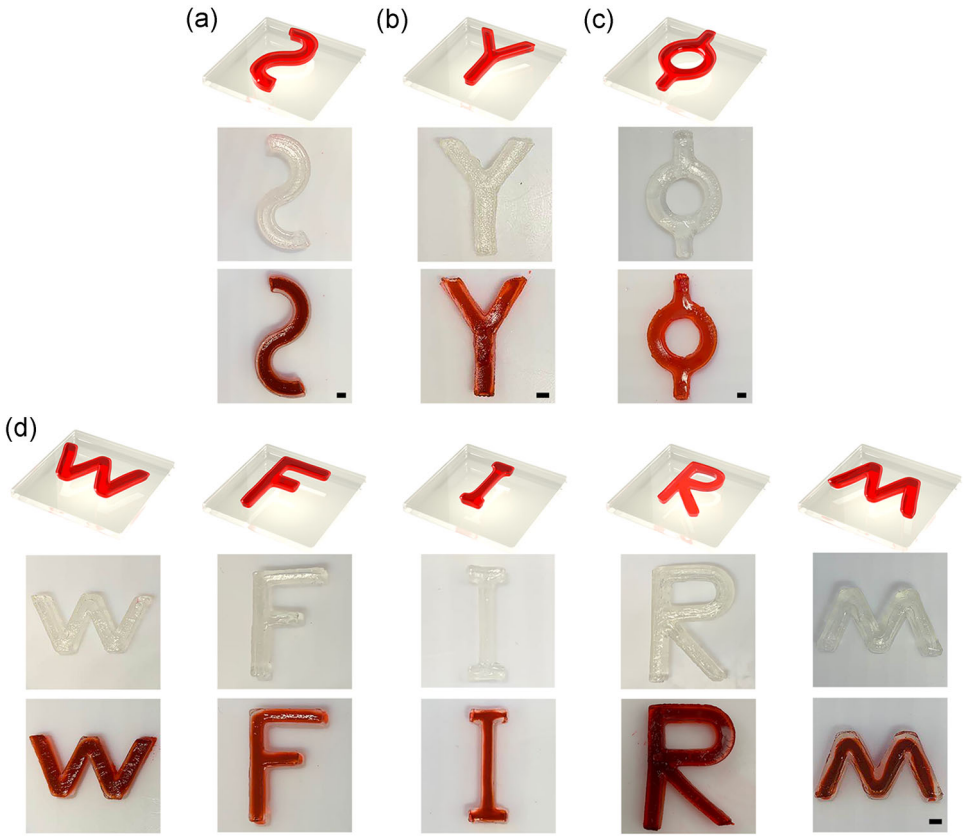

FIGURE 4 Three-dimensional complex tubular structure made by two-step crosslinking method. (a–c) Multiple curved, branched, and circular tubular structure with single inlet/outlet. (d) Printed letter with tubular structure. All structures were injected with a red ink for the approval of good sealing and patency. Scale bar = 2 mm

and additive manufacturing technology, which considers various design aspects such as imaging, modeling, printer selection, bioink selection, culture conditions, and 3D structure (Murphy & Atala, 2014; Y. S. Zhang et al., 2018). However, there are still difficulties in the fabrication of complicated SDBVs. The medical application of 3D printing technology is still limited, especially due to that available bioinks are not suitable for the most targeted applications. Printable materials with good biocompatibility tend to have poor mechanical properties. During the printing process, the collapse of structure due to gravity is one of the common causes that lead to fabrication failure (Ozbolat & Hospodiuk, 2016).

Normally, sacrificial hydrogels offer a temporary support in the fabrication of small-diameter vessels. But all sacrificial hydrogels have disadvantages (Bertassoni et al., 2014; Tocchio et al., 2015). Therefore, we developed a two-step crosslinking method to fabricate tunable structures. This method avoids the use of sacrificial hydrogels and produces a vessel structure with using single photocurable hydrogel—GelMA without using sacrificial hydrogels.

Hydrogel, as a material for loading cells and supporting structures, is particularly important in 3D bioprinting (Hoelzl et al., 2016). An ideal hydrogel needs to have biological and mechanical properties close to its intended tissue and should be adaptable to the printing process. In addition, hydrogel structures need to facilitate cell proliferation and differentiation after bioprinting. Naturally derived hydrogels, including agarose, alginate, collagen, fibrin, gelatin, and HA, provide an effective growth environment for cells (Cui et al., 2017). However, these hydrogels lack sufficient mechanical strength to create the complicated 3D tubular structure. GelMA as a biocompatible polymer is produced by modified gelatin with MA, and is able to be crosslinked with UV light to obtain higher physical strength (Liu & Chan-Park, 2010). Our preliminary experiments showed that crosslinked GelMA hydrogel can be stacked up to 20 printed layers. In this study, 5% (m/v) GelMA was used to fabricate the tubular structure. The pore size at this concentration could hold SMCs in the spot of 3D space, and was beneficial to the proliferation of the cells (Jeong et al., 2007). We compared the properties of GelMA solution with different curing time. Although GelMA with 5 s crosslinking time could get semisolid immediately, it could not keep its shape for a longer time. The MA group in GelMA will open continuously and form connectivity during the extension of crosslinking time. The storage modulus, viscosity coefficient, and residual mass of GelMA will be increased, while the expansion radio will be decreased due to the process of crosslinking. With the crosslinking agent that we used in the study, 5% GelMA can achieve complete crosslinked state basically under 40 s UV light with a wavelength of 365 nm and the intensity of 200 mV/cm^2, and then it

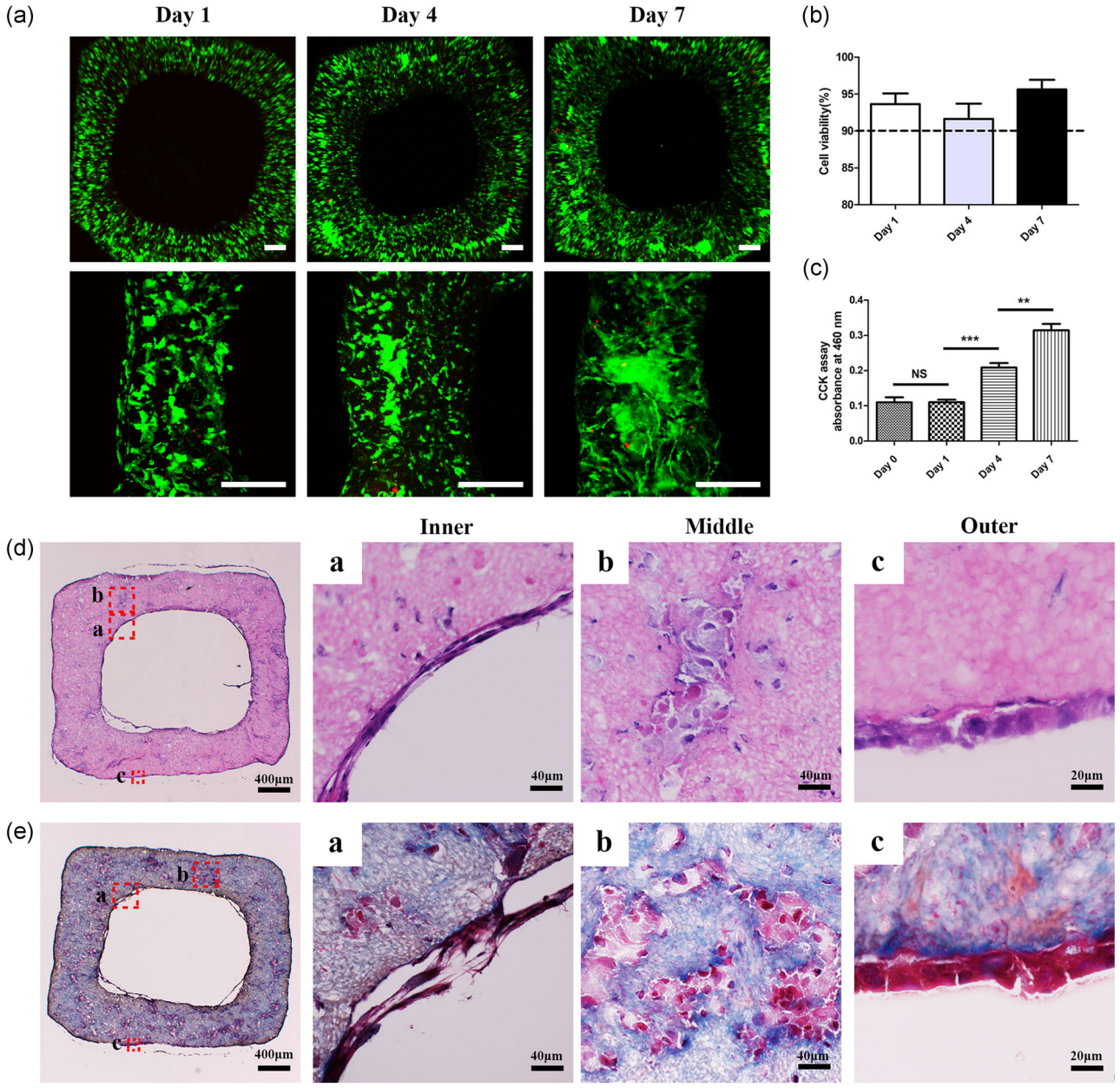

FIGURE 5 Cell viability, proliferation, and histology of bionic vascular vessel. (a) Live/dead staining of bionic vascular vessel (Day 1, Day 4, and Day 7). Scale bar = 200 μm. (b) Cell viability of bionic vascular. (c) Cell proliferation by CCK-8 assay ($n = 4$, $^{**}p < 0.01$; $^{***}p < 0.001$). (d, e) The H&E staining and Masson staining. CCK-8, Cell Counting Kit-8; H&E, hematoxylin and eosin; NS, not significant

remains in a stable state with the extension of crosslinking time. The 10 s crosslinking time for GelMA was chosen at the first crosslinking step to ensure the stability of the transfer structure, open the least double bonds, and then lay a proper foundation for the second crosslinking step. In our results, two independent structures can be well connected with the 10 s as the first crosslinking step. The comparison of the structures fabricated by one-step and two-step method indicates that there is no obvious difference in microstructure and mechanical properties. Moreover, the water absorption capacity of GelMA with 5 s and 10 s crosslinking time could reach 400 times of its own mass in DI water, and its volume also expands accordingly. Therefore, the low degree of crosslinked GelMA was also a good swelling material to be applied in the research field of tissue engineering.

Precrosslinking can enhance the physical property of photocurable hydrogel. In the process of vertical bioprinting, the printed bottom GelMA bioink was partly crosslinked by continuous UV light to avoid cell leakage and structure collapse (Xu et al., 2020). A user-defined, complexity cell-laden channel was fabricated by a sequential printing approach. The photocurable hydrogels were briefly exposed layer-by-layer to increase support performance. The sacrificial hydrogels were printed into the desired layer and fully crosslinked.

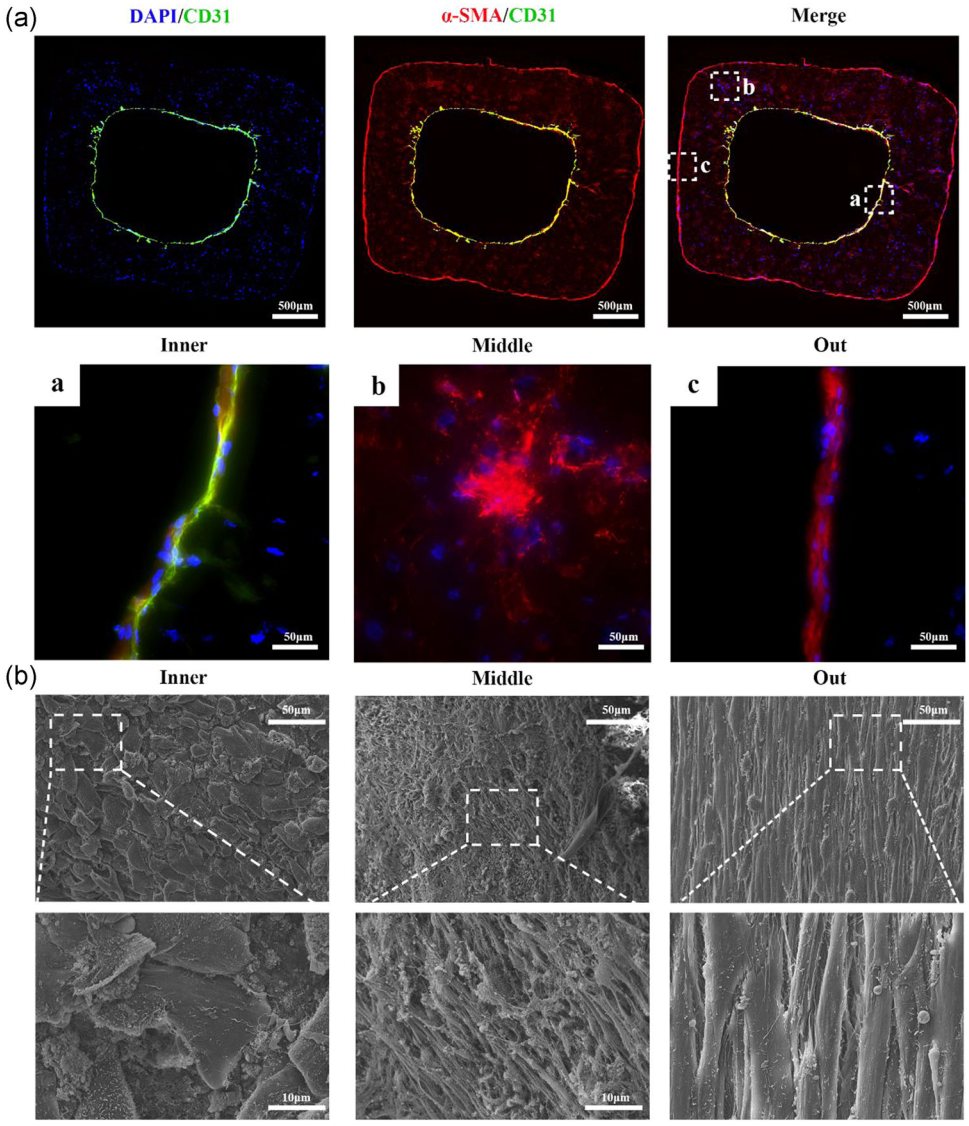

FIGURE 6 Immunofluorescence and SEM of bionic vascular vessel. (a) Immunofluorescence of bionic vascular vessel (CD31, green; α-SMA, red; DAPI, blue). (b) SEM of bionic vascular vessel. HUVECs attached on the intraluminal surface, and SMCs were distributed linearly within the wall of the structure. DAPI, 4′,6-diamidino-2-phenylindole; HUVEC, human umbilical vein endothelial cell; SEM, scanning electron microscope; SMC, smooth muscle cell; α-SMA, α-smooth muscle actin

With the removal of sacrificial hydrogels, precise and complex channels could be constructed (Ji et al., 2019). In our study, GelMA was made semisolid after first-step crosslinking process. The semisolid GelMA with required physical strength could be bonded tightly with uncrosslinked GelMA. The combination was received second-step crosslinking process which produced a longer UV exposure time. A bionic vascular vessel with small diameter was built successfully with using the two-step crosslinking method, which maintains consecutive tubular structure. The cross-section of printed tubular structure was quadrate. In our subsequent investigation, we will assemble two semicircle structures into a circular tubular structure by this method and construct bionic blood vessels that are more in line with vascular anatomy and dynamics.

Furthermore, this method might be not only suitable for vessels, but also for other complicated structures, such as hepatic sinusoid, nephron, and pulmonary alveoli. The hydrogel can be partly cured, and the two-step curing can integrate two independent parts into a whole. The two-step crosslinking method may be suitable to photocurable hydrogel with better mechanical properties and make structures that are difficult to be formed by one-step crosslinking method. In addition, different kinds of photocuring materials containing double bonds may also be used with this two-step crosslinking method. In this way, we could make the connection between different tissues in bioprinting, such as the superior vena cava bioprinted by one photocuring material connects with the heart which is bioprinted by another photocuring material.

Human blood vascular vessel have three distinct layers: intima (endothelial cells), media (SMCs), and externa (fibroblasts) (Tomasina et al., 2019). We created a small-diameter vascular structure (Ø < 6 mm) with the spatial distribution of two different cells, which include bioprinted SMCs within bioink and subsequent perfusion of HUVECs into the lumen space. SMCs could aggregate, spread out, and proliferate to form outer layer of the construct, and rich collagen area was found in that area. Perfused HUVECs formed the connected inner layer that covers entire intralumenal surface with dense junctions. The SMCs were lined longitudinally along the structure which may be caused by axial traction during printing. During the culture of bioprinted vessel structure, the previous inner square shape turned to smooth gradually, that has been reported in previously publication (Esch et al., 2011).

Through this two-step crosslinking method, we have successfully bioprinted multiple complicated tubular structures and bionics vessels with inner monolayer endothelium surrounded by outer layer SMCs. This new fabrication method for tissue engineering of small-diameter vessel might be applied in developing small blood vessel for clinical application. In addition, two-step crosslinking method could be adopted to create more complex structures that are implantable and functional for the alternative therapies.

5 | CONCLUSION

We proposed a new approach to making small-diameter vessels with complicated patterns and spatial cell distribution. The two-step crosslinking method created a continuous connection between different printed parts and resulted an intact tubular structure with biological and mechanical advantages. We accomplished this method through the investigation of GelMA properties altered by crosslinking time and optimized by crosslinking process. We fabricated a small vessel that possesses printed outer layer of SMCs and perfused inner layer of HUVECs by using GelMA bioink and two-step crosslinking method. We also observed that the SMCs and HUVECs were proliferated, and functionalized during postprinting culture. Our study might provide a new fabrication method for the construction of small-diameter vessel with clinically relevant size and characteristics.

ACKNOWLEDGMENTS

This study was mainly supported by the translation grant from the State of North Carolina, USA, the National Natural Science Foundation of China (31900969), Suzhou Municipal Science and Technology Bureau (SYS2020071), Suzhou Science and Education for Healthy (KJXW2019073), and the Gusu Health Talent Training Project of Suzhou (GSWS2019088).

CONFLICT OF INTERESTS

The authors declare no conflict of interest.

AUTHOR CONTRIBUTIONS

Weixin Zhao and Anthony Atala conceived and supervised the study. Weixin Zhao and Ruixin Hou designed experiments. Qianheng Jin performed experiments. Qianheng Jin and Guangzhe Jin wrote the manuscript. Weixin Zhao revised the manuscript. Guangzhe Jin, Jihui Ju, Lei Xu, Linfeng Tang, and Yi Fu analyzed data, and commented on the manuscript.

DATA AVAILABILITY STATEMENT

The data that support the findings of this study are available from the corresponding author upon reasonable request.

ORCID

Qianheng Jin http://orcid.org/0000-0001-5108-7992

REFERENCES

Bahcecioglu, G., Hasirci, N., Bilgen, B., & Hasirci, V. (2019). A 3D printed PCL/hydrogel construct with zone-specific biochemical composition mimicking that of the meniscus. *Biofabrication*, *11*(2):025002. https://doi.org/10.1088/1758-5090/aaf707

Bertassoni, L. E., Cecconi, M., Manoharan, V., Nikkhah, M., Hjortnaes, J., Cristino, A. L., Barabaschi, G., Demarchi, D., Dokmeci, M. R., Yang, Y., & Khademhosseini, A. (2014). Hydrogel bioprinted microchannel networks for vascularization of tissue engineering constructs. *Lab on a Chip*, *14*(13), 2202–2211. https://doi.org/10.1039/c4lc00030g

Buchanan, G. L., Chieffo, A., Meliga, E., Mehran, R., Park, S. J., Onuma, Y., Capranzano, P., Valgimigli, M., Narbute, I., Makkar, R. R., Palacios, I. F., Kim, Y. H., Buszman, P. P., Chakravarty, T., Sheiban, I., Naber, C., Margey, R., Agnihotri, A., Marra, S., … Colombo, A. (2014). Comparison of percutaneous coronary intervention (with drug-eluting stents) versus coronary artery bypass grafting in women with severe narrowing of the left main coronary artery (from the Women-Drug-Eluting stent for LefT main coronary Artery disease Registry). *American Journal of Cardiology*, *113*(8), 1348–1355. https://doi.org/10.1016/j.amjcard.2014.01.409

Chen, Y. C., Lin, R. Z., Qi, H., Yang, Y., Bae, H., Melero-Martin, J. M., & Khademhosseini, A. (2012). Functional human vascular network generated in photocrosslinkable gelatin methacrylate hydrogels. *Advanced Functional Materials*, *22*(10), 2027–2039. https://doi.org/10.1002/adfm.201101662

Cui, H., Nowicki, M., Fisher, J. P., & Zhang, L. G. (2017). 3D bioprinting for organ regeneration. *Advanced Healthcare Materials*, *6*(1):1601118. https://doi.org/10.1002/adhm.201601118

Cui, H., Zhu, W., Huang, Y., Liu, C., Yu, Z. X., Nowicki, M., Miao, S., Cheng, Y., Zhou, X., Lee, S. J., Zhou, Y., Wang, S., Mohiuddin, M., Horvath, K., & Zhang, L. G. (2019). In vitro and in vivo evaluation of 3D bioprinted small-diameter vasculature with smooth muscle and endothelium. *Biofabrication*, *12*(1):015004. https://doi.org/10.1088/1758-5090/ab402c

Dursun Usal, T., Yucel, D., & Hasirci, V. (2019). A novel GelMA-pHEMA hydrogel nerve guide for the treatment of peripheral nerve damages. *International Journal of Biological Macromolecules*, *121*, 699–706. https://doi.org/10.1016/j.ijbiomac.2018.10.060

Elliott, M. B., & Gerecht, S. (2016). Three-dimensional culture of small-diameter vascular grafts. *Journal of Materials Chemistry B: Materials for Biology and Medicine*, *4*(20), 3443–3453. https://doi.org/10.1039/c6tb00024j

Esch, M. B., Post, D. J., Shuler, M. L., & Stokol, T. (2011). Characterization of in vitro endothelial linings grown within microfluidic channels. *Tissue Engineering. Part A*, *17*(23–24), 2965–2971. https://doi.org/10.1089/ten.tea.2010.0371

Freeman, S., Ramos, R., Alexis Chando, P., Zhou, L., Reeser, K., Jin, S., Soman, P., & Ye, K. (2019). A bioink blend for rotary 3D bioprinting tissue engineered small-diameter vascular constructs. *Acta Biomaterialia*, *95*, 152–164. https://doi.org/10.1016/j.actbio.2019.06.052

Hoelzl, K., Lin, S., Tytgat, L., Van Vlierberghe, S., Gu, L., & Ovsianikov, A. (2016). Bioink properties before, during and after 3D bioprinting. *Biofabrication*, *8*(3):032002. https://doi.org/10.1088/1758-5090/8/3/032002

Hong, H., Seo, Y. B., Kim, D. Y., Lee, J. S., Lee, Y. J., Lee, H., Ajiteru, O., Sultan, M. T., Lee, O. J., Kim, S. H., & Park, C. H. (2020). Digital light processing 3D printed silk fibroin hydrogel for cartilage tissue engineering. *Biomaterials*, *232*, 119679. https://doi.org/10.1016/j.biomaterials.2019.119679

Jeong, S. I., Kim, S. Y., Cho, S. K., Chong, M. S., Kim, K. S., Kim, H., Lee, S. B., & Lee, Y. M. (2007). Tissue-engineered vascular grafts composed of marine collagen and PLGA fibers using pulsatile perfusion bioreactors. *Biomaterials*, *28*(6), 1115–1122. https://doi.org/10.1016/j.biomaterials.2006.10.025

Ji, S., Almeida, E., & Guvendiren, M. (2019). 3D bioprinting of complex channels within cell-laden hydrogels. *Acta Biomaterialia*, *95*, 214–224. https://doi.org/10.1016/j.actbio.2019.02.038

Jing, X., Mi, H. Y., Salick, M. R., Cordie, T. M., Peng, X. F., & Turng, L. S. (2015). Electrospinning thermoplastic polyurethane/graphene oxide scaffolds for small diameter vascular graft applications. *Materials Science and Engineering C: Materials for Biological Applications*, *49*, 40–50. https://doi.org/10.1016/j.msec.2014.12.060

Kolesky, D. B., Homan, K. A., Skylar-Scott, M. A., & Lewis, J. A. (2016). Three-dimensional bioprinting of thick vascularized tissues. *Proceedings of the National Academy of Sciences of the United States of America*, *113*(12), 3179–3184. https://doi.org/10.1073/pnas.1521342113

Kolesky, D. B., Truby, R. L., Gladman, A. S., Busbee, T. A., Homan, K. A., & Lewis, J. A. (2014). 3D bioprinting of vascularized, heterogeneous cell-laden tissue constructs. *Advanced Materials*, *26*(19), 3124–3130. https://doi.org/10.1002/adma.201305506

Lesman, A., Rosenfeld, D., Landau, S., & Levenberg, S. (2016). Mechanical regulation of vascular network formation in engineered matrices. *Advanced Drug Delivery Reviews*, *96*, 176–182. https://doi.org/10.1016/j.addr.2015.07.005

Liu, Y., & Chan-Park, M. B. (2010). A biomimetic hydrogel based on methacrylated dextran-graft-lysine and gelatin for 3D smooth muscle cell culture. *Biomaterials*, *31*(6), 1158–1170. https://doi.org/10.1016/j.biomaterials.2009.10.040

Miller, J. S., Stevens, K. R., Yang, M. T., Baker, B. M., Nguyen, D. H., Cohen, D. M., Toro, E., Chen, A. A., Galie, P. A., Yu, X., Chaturvedi, R., Bhatia, S. N., & Chen, C. S. (2012). Rapid casting of patterned vascular networks for perfusable engineered three-dimensional tissues. *Nature Materials*, *11*(9), 768–774. https://doi.org/10.1038/nmat3357

Morin, K. T., Smith, A. O., Davis, G. E., & Tranquillo, R. T. (2013). Aligned human microvessels formed in 3D fibrin gel by constraint of gel contraction. *Microvascular Research*, *90*, 12–22. https://doi.org/10.1016/j.mvr.2013.07.010

Murphy, S. V., & Atala, A. (2014). 3D bioprinting of tissues and organs. *Nature Biotechnology*, *32*(8), 773–785. https://doi.org/10.1038/nbt.2958

Nemeno-Guanzon, J. G., Lee, S., Berg, J. R., Jo, Y. H., Yeo, J. E., Nam, B. M., Koh, Y. G., & Lee, J. I. (2012). Trends in tissue engineering for blood vessels. *Journal of Biomedicine and Biotechnology*, *2012*, 956345. https://doi.org/10.1155/2012/956345

Norotte, C., Marga, F. S., Niklason, L. E., & Forgacs, G. (2009). Scaffold-free vascular tissue engineering using bioprinting. *Biomaterials*, *30*(30), 5910–5917. https://doi.org/10.1016/j.biomaterials.2009.06.034

Ozbolat, I. T., & Hospodiuk, M. (2016). Current advances and future perspectives in extrusion-based bioprinting. *Biomaterials*, *76*, 321–343. https://doi.org/10.1016/j.biomaterials.2015.10.076

Pattanaik, S., Arbra, C., Bainbridge, H., Dennis, S. G., Fann, S. A., & Yost, M. J. (2019). Vascular tissue engineering using scaffold-free prevascular endothelial-fibroblast constructs. *BioResearch Open Access*, *8*(1), 1–15. https://doi.org/10.1089/biores.2018.0039

Rodriguez, A. E., Pavlovsky, H., & Del Pozo, J. F. (2016). Understanding the outcome of randomized trials with drug-eluting stents and coronary artery bypass graft in patients with multivessel disease: A review of a 25-year journey. *Clinical Medicine Insights. Cardiology*, *10*, 195–199. https://doi.org/10.4137/CMC.S40645

Tocchio, A., Tamplenizza, M., Martello, F., Gerges, I., Rossi, E., Argentiere, S., Rodighiero, S., Zhao, W., Milani, P., & Lenardi, C. (2015). Versatile fabrication of vascularizable scaffolds for large tissue engineering in bioreactor. *Biomaterials*, *45*, 124–131. https://doi.org/10.1016/j.biomaterials.2014.12.031

Tomasina, C., Bodet, T., Mota, C., Moroni, L., & Camarero-Espinosa, S. (2019). Bioprinting vasculature: Materials, cells and emergent techniques. *Materials (Basel)*, *12*(17):2701. https://doi.org/10.3390/ma12172701

de Vries, M. R., Simons, K. H., Jukema, J. W., Braun, J., & Quax, P. H. (2016). Vein graft failure: From pathophysiology to clinical outcomes. *Nature Reviews Cardiology*, *13*(8), 451–470. https://doi.org/10.1038/nrcardio.2016.76

Wang, W., Nie, W., Zhou, X., Feng, W., Chen, L., Zhang, Q., You, Z., Shi, Q., Peng, C., & He, C. (2018). Fabrication of heterogeneous porous bilayered nanofibrous vascular grafts by two-step phase separation technique. *Acta Biomaterialia*, *79*, 168–181. https://doi.org/10.1016/j.actbio.2018.08.014

Wu, W., DeConinck, A., & Lewis, J. A. (2011). Omnidirectional printing of 3D microvascular networks. *Advanced Materials*, *23*(24), H178–H183. https://doi.org/10.1002/adma.201004625

Xu, L., Varkey, M., Jorgensen, A., Ju, J., Jin, Q., Park, J. H., Fu, Y., Zhang, G., Ke, D., Zhao, W., Hou, R., & Atala, A. (2020). Bioprinting small diameter blood vessel constructs with an endothelial and smooth muscle cell bilayer in a single step. *Biofabrication*, *12*(4):045012. https://doi.org/10.1088/1758-5090/aba2b6

Yamanaka, H., Yamaoka, T., Mahara, A., Morimoto, N., & Suzuki, S. (2018). Tissue-engineered submillimeter-diameter vascular grafts for free flap survival in rat model. *Biomaterials*, *179*, 156–163. https://doi.org/10.1016/j.biomaterials.2018.06.022

Zhang, Y., Li, X. S., Guex, A. G., Liu, S. S., Müller, E., Malini, R. I., Zhao, H. J., Rottmar, M., Maniura-Weber, K., Rossi, R. M., & Spano, F. (2017). A compliant and biomimetic three-layered vascular graft for small blood vessels. *Biofabrication*, *9*(2):025010. https://doi.org/10.1088/1758-5090/aa6bae

Zhang, Y. S., Oklu, R., Dokmeci, M. R., & Khademhosseini, A. (2018). Three-dimensional bioprinting strategies for tissue engineering. *Cold Spring Harbor Perspectives in Medicine*, *8*(2):a025718. https://doi.org/10.1101/cshperspect.a025718

Zoghbi, W. A., Duncan, T., Antman, E., Barbosa, M., Champagne, B., Chen, D., Gamra, H., Harold, J. G., Josephson, S., Komajda, M., Logstrup, S., Mayosi, B. M., Mwangi, J., Ralston, J., Sacco, R. L., Sim, K. H., Smith Jr., S. C., Vardas, P. E., & Wood, D. A. (2014). Sustainable development goals and the future of cardiovascular health: A statement from the Global Cardiovascular Disease Taskforce. *Global Heart*, *9*(3), 273–274. https://doi.org/10.1016/j.gheart.2014.09.003

SUPPORTING INFORMATION

Additional supporting information may be found in the online version of the article at the publisher's website.

How to cite this article: Jin, Q., Jin, G., Ju, J., Xu, L., Tang, L., Fu, Y., Hou, R., Atala, A., & Zhao, W. (2022). Bioprinting small-diameter vascular vessel with endothelium and smooth muscle by the approach of two-step crosslinking process. *Biotechnology and Bioengineering*, 119, 1673–1684. https://doi.org/10.1002/bit.28075